Journal of Spacecraft and Rockets
Vol. 35, No. 4, July–August 1998

Low-Thrust Inclination Control in Presence of Earth Shadow

Jean Albert Kechichian*
The Aerospace Corporation, El Segundo, California 90245-4691

The problem of inclination change in near-circular orbit using intermittent, low-thrust solar electric propulsion is analyzed. Given the shadow arc length and the line of nodes of initial to final orbits, piecewise constant yaw angles are selected, and the location along the orbit where the yaw angle switches is optimized to carry out the largest inclination change per revolution for that particular geometry. Single-switch and two-switch strategies are analyzed, and several algorithms of varying complexity are described and numerically tested for their relative performance. This approach yields suboptimal but robust and real-time autonomous onboard guidance software for electric orbit transfer vehicle orbital transfer applications.

Nomenclature

a_0	= semimajor axis of reference orbit, km
f	= thrust magnitude
$\boldsymbol{f}$	= acceleration vector due to thrust
f_r, f_θ, f_h	= components of acceleration vector along $\hat{r}, \hat{\theta}, \hat{h}$ Euler–Hill directions
h	= orbital angular momentum, km^2/s
$\hat{\boldsymbol{h}}$	= unit vector along instantaneous angular momentum vector $\boldsymbol{h}$
m	= spacecraft mass
n	= mean motion of reference orbit, $(\mu/a_0^3)^{1/2}$, rad/s
$\boldsymbol{r}$	= spacecraft position vector, Earth centered
$\hat{\boldsymbol{r}}$	= unit vector along instantaneous radius vector $\boldsymbol{r}$
$s_{\theta'}, c_{\theta'}$	= $\sin\theta'$, $\cos\theta'$, etc.
$\boldsymbol{T}$	= thrust vector
$\hat{\boldsymbol{x}}, \hat{\boldsymbol{y}}$	= unit vectors along the inertial x and y directions
θ'	= spacecraft angular position at time t measured from x axis
$\hat{\boldsymbol{\theta}}$	= unit vector in instantaneous orbit plane, perpendicular to $\hat{\boldsymbol{r}}$
θ_h	= out-of-plane or thrust yaw angle
θ_t	= thrust pitch angle
μ	= gravity constant of Earth, 398,601.3 km^3/s^2
τ	= nondimensional time

Introduction

THE problem of low-thrust transfer between inclined circular orbits benefited from the contributions of Edelbaum[1] and Wiesel and Alfano,[2] who provided analytic solutions to execute minimum-time transfers using continuous constant or variable acceleration and constant or optimized yaw profile within each revolution. Cass[3] and McCann[4] provided semianalytic solutions of the optimal thrust pitch and yaw profiles for transfers using intermittent thrusting due to shadowing. A simulation tool was developed[5] using simplifying assumptions to carry out preliminary parametric studies as well as spacecraft systems design and optimization assessments. Analytic solutions leading to suboptimal transfers were developed[6,7] for possible implementation in fast computer programs similar to the one depicted in Ref. 5. Many of these analytic methods assume that the orbit remains circular during the transfer for ease of calculation of various dynamic and geometric parameters during the generation of the transfer solution. Higher-fidelity simulations using averaging techniques are described with optimized pitch and yaw profiles and intermittent thrusting due to shadowing.[8–10] These simulations show that the intermediate orbits' eccentricities remain below 0.2 for the worst case of shadowing geometry for typical low-Earth-orbit (LEO) to geostationary-Earth-orbit transfers. However, these numerically generated transfers are difficult to obtain and therefore are not suitable for parametric studies, which require a great number of iterations. In view of the small eccentricity buildup and the need to use simple but efficient control strategies easily implemented in analytic-type codes, the control problem for inclination change in the presence of Earth shadow is approached in this paper from a purely analytic but suboptimal point of view. Marec[11] shows several optimal thrust acceleration laws for various low-thrust systems applicable in general elliptic orbits with no restrictions as to the location of the thrust arcs. In our problem, the acceleration magnitude is assumed to remain constant and the orbit circular.

Thus, pure inclination change in near-circular orbit using low thrust is analyzed for solar electric propulsion systems using intermittent thrust along the orbit. The continuous-thrust solutions are such that the out-of-plane thrust angle or the yaw angle switches between ±90 deg every half orbit, with the switch points located at the antinodes. These results are extended to the case in which an eclipse or shadow arc restricts thrusting in sunlight only, so that thrusting is now intermittent during each orbit. Given an arbitrarily selected line of nodes of initial to final orbits and given the length of the shadow arc, simple but robust algorithms are presented that effect the largest change in inclination during the revolution by thrusting only in sunlight. The geometry of the problem is illustrated in Fig. 1, where the Earth-centered inertial x, y frame is such that x is pointing toward the point on the orbit corresponding to exit from shadow. The line of nodes is inclined with respect to the x axis by the angle β, where β can be anywhere between 0 and 360 deg. Furthermore, the arc OO′ is the sunlit arc where thrusting is allowed, and the arc O′O is the shadowed arc where thrusting is not possible. The shadow geometry is calculated easily once the sun look angle β_s is evaluated from the knowledge of the solar right ascension and declination as well as the spacecraft orbit equatorial inclination and ascending node. The node is allowed to regress because of J_2, and the amount by which Ω changes is calculated from the analytic expression defining the regression rate. This rate is dependent on the orbital equatorial inclination as well as the orbital semimajor axis. The angle β_s therefore must be updated from revolution to subsequent revolution and the x axis repositioned to point toward the current exit from shadow to effect the orbit rotation calculations during that particular revolution, following the algorithms presented in the following sections. We analyze both single-switch and two-switch strategies while holding the yaw angle constant between two switches.

Analysis

The variation-of-parameters equations linearized about a reference circular orbit, representing the initial circular orbit, are a complete set of first-order differential equations that describe the

Presented as Paper 91-157 at the AAS/AIAA Spaceflight Mechanics Meeting, Houston, TX, Feb. 11–13, 1991; received Aug. 22, 1997; revision received Jan. 28, 1998; accepted for publication Feb. 9, 1998.

*Engineering Specialist, Astrodynamics Department, MS M4/947, P.O. Box 92957, Los Angeles, CA 90009. E-mail: Jean.A.Kechichian@aero.org. Associate Fellow AIAA.

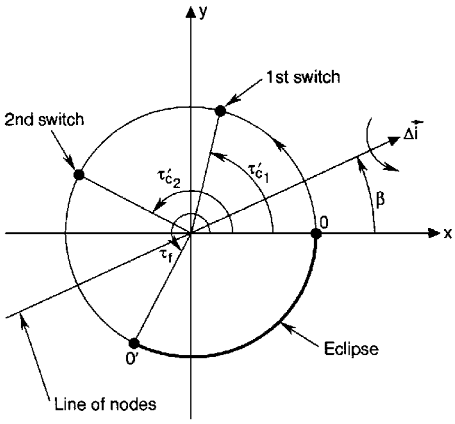

Fig. 1 Orbit transfer and switch geometry.

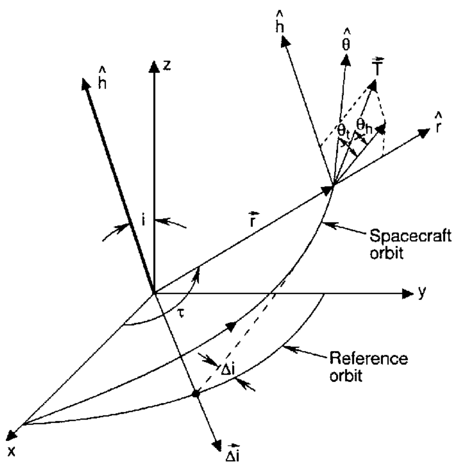

Fig. 2 Euler–Hill frame and thrust geometry.

motion of the thrusting spacecraft. The pertinent equations that describe the out-of-plane motion consist of

$$\frac{\mathrm{d}\Delta i_x}{\mathrm{d}\tau} = \frac{a_0^2}{\mu} c_{\theta'} f_h \tag{1}$$

$$\frac{\mathrm{d}\Delta i_y}{\mathrm{d}\tau} = \frac{a_0^2}{\mu} s_{\theta'} f_h \tag{2}$$

The change in the inclination $\boldsymbol{\Delta i}$ along the line of nodes is a vector with components Δi_x and Δi_y along the x and y directions as in Fig. 1. The rates are with respect to the nondimensional time $\tau = nt$, where n is the reference-orbit mean motion corresponding to the semimajor axis a_0. Given the $\hat{\boldsymbol{x}}, \hat{\boldsymbol{y}}$ plane of the initial reference circular orbit of semimajor axis a_0 and mean motion n, $\boldsymbol{\Delta i} = \Delta i_x \hat{\boldsymbol{x}} + \Delta i_y \hat{\boldsymbol{y}}$, where $\Delta i_x = \Delta i c_{\theta'}$ and $\Delta i_y = \Delta i s_{\theta'}$, with the magnitude Δi obtained from the variation-of-parameters equation

$$\frac{\mathrm{d}i}{\mathrm{d}t} = \left(\frac{r f_h}{h}\right) c_\theta$$

with θ representing the angular position of the spacecraft measured from the ascending node. The spacecraft being initially on the reference circular orbit, $\theta = 0$, $r = a_0$, $h = n a_0^2$ such that Δi due to a small impulse $\boldsymbol{\Delta V}$ applied along the direction $\boldsymbol{\alpha} = (\alpha_r, \alpha_\theta, \alpha_h)$ is given by $\Delta i = (\Delta V / n a_0) \alpha_h$ due to $\Delta t f_h = \Delta V \alpha_h$. Finally, $\boldsymbol{\Delta i} = (\Delta V / n a_0) \alpha_h \hat{\boldsymbol{r}}$, $\Delta i_x = (\Delta V / n a_0) \alpha_h c_{\theta'}$, $\Delta i_y = (\Delta V / n a_0) \alpha_h s_{\theta'}$. The nondimensional rates in Eqs. (1) and (2) are now obtained because $h^2/\mu = a_0$ for a nominally circular orbit, and $\theta' \simeq nt = \tau$. Figure 2 shows the spacecraft at position $\boldsymbol{r}$ with respect to the center of the Earth, with $\boldsymbol{T}$ such that θ_h is the angle between this thrust vector and its projection in the $(\hat{\boldsymbol{r}}, \hat{\boldsymbol{\theta}})$ plane and θ_t is the angle between this projection and the $\hat{\boldsymbol{\theta}}$ direction. Assuming that the instantaneous osculating orbit never departs from the near-circular shape, it is then possible to use the approximation mentioned earlier, $\theta' \simeq nt = \tau$, $c_{\theta'} \simeq c_\tau$, and $s_{\theta'} \simeq s_\tau$, such that, with $k = f/m$, the linearized Eqs. (1) and (2) can now be written as

$$\frac{\mathrm{d}\Delta i_x}{\mathrm{d}\tau} = \frac{k}{a_0 n^2} c_\tau s_{\theta_h} \tag{3}$$

$$\frac{\mathrm{d}\Delta i_y}{\mathrm{d}\tau} = \frac{k}{a_0 n^2} s_\tau s_{\theta_h} \tag{4}$$

If θ_h is assumed to be piecewise constant, then Eqs. (3) and (4) can be integrated analytically between $\tau = 0$ and $\tau = \tau_f$ (Fig. 1). Let us first analyze the single-switch strategy, and let τ'_c correspond to the switch angular position. Then, if θ_{h_1} is the constant yaw angle between $\tau = 0$ and $\tau = \tau'_c$ and θ_{h_2} is the yaw angle between $\tau = \tau'_c$ and $\tau = \tau_f$,

$$\Delta i_x = g s_{\theta_{h_1}} \int_0^{\tau'_c} c_\tau \,\mathrm{d}\tau + g s_{\theta_{h_2}} \int_{\tau'_c}^{\tau_f} c_\tau \,\mathrm{d}\tau \tag{5}$$

$$\Delta i_y = g s_{\theta_{h_1}} \int_0^{\tau'_c} s_\tau \,\mathrm{d}\tau + g s_{\theta_{h_2}} \int_{\tau'_c}^{\tau_f} s_\tau \,\mathrm{d}\tau \tag{6}$$

The constant g represents a normalized acceleration with $g = k/(a_0 n^2)$. Carrying out the integration results in

$$\Delta i_x = g s_{\tau'_c} s_{\theta_{h_1}} + g\left(s_{\tau_f} - s_{\tau'_c}\right) s_{\theta_{h_2}} = \Delta i c_\beta \tag{7}$$

$$\Delta i_y = -g\left(c_{\tau'_c} - 1\right) s_{\theta_{h_1}} - g\left(c_{\tau_f} - c_{\tau'_c}\right) s_{\theta_{h_2}} = \Delta i s_\beta \tag{8}$$

These two equations can be solved simultaneously to provide the θ_{h_1} and θ_{h_2} angles for given Δi, β, τ'_c, and τ_f as well as g:

$$s_{\theta_{h_1}} = \frac{\Delta i \left(c_{\beta - \tau'_c} - c_{\beta - \tau_f}\right)}{g\left(s_{\tau_f - \tau'_c} + s_{\tau'_c} - s_{\tau_f}\right)} \tag{9}$$

$$s_{\theta_{h_2}} = \frac{\Delta i \left(c_{\beta - \tau'_c} - c_\beta\right)}{g\left(s_{\tau_f - \tau'_c} + s_{\tau'_c} - s_{\tau_f}\right)} \tag{10}$$

Equations (9) and (10) uniquely define θ_{h_1} and θ_{h_2} because $-\pi/2 \le \theta_{h_1} \le \pi/2$ and $-\pi/2 \le \theta_{h_2} < \pi/2$ such that $|s_{\theta_{h_1}}| \le 1$ and $|s_{\theta_{h_2}}| \le 1$ or $s^2_{\theta_{h_1}} \le 1$ and $s^2_{\theta_{h_2}} \le 1$; Δi is the magnitude of the inclination change and is therefore a positive quantity. The constant g is also strictly positive. The largest eclipse arc in LEO never exceeds 140 deg, so that 220 deg $\le \tau_f \le$ 360 deg. This, in turn, requires that $s_{\tau_f} \le 0$. It now can be shown that the factor in the denominator, namely $(s_{\tau_f - \tau'_c} + s_{\tau'_c} - s_{\tau_f}) \ge 0$, is positive semidefinite. From

$$s_{\tau_f - \tau'_c} + s_{\tau'_c} - s_{\tau_f} \ge 0 \tag{11}$$

it follows that

$$s_{\tau'_c}\left(1 - c_{\tau_f}\right) - s_{\tau_f}\left(1 - c_{\tau'_c}\right) \ge 0$$

Both $(1 - c_{\tau_f})$ and $(1 - c_{\tau'_c})$ are ≥ 0, and with $s_{\tau_f} \le 0$, the condition in Eq. (11) is equivalent to

$$s_{\tau'_c} \ge \frac{s_{\tau_f}\left(1 - c_{\tau'_c}\right)}{\left(1 - c_{\tau_f}\right)} \tag{12}$$

where the right-hand side is ≤ 0. If $s_{\tau'_c} \ge 0$, then the inequality in Eq. (12) is always satisfied. If $s_{\tau'_c} \le 0$, then Eq. (12) can be written as

$$s_{\tau'_c}\left(1 - c_{\tau_f}\right) \ge s_{\tau_f}\left(1 - c_{\tau'_c}\right)$$

where the right- and left-hand sides are ≤ 0. Squaring, one has

$$s^2_{\tau'_c}\left(1 - c_{\tau_f}\right)^2 \ge s^2_{\tau_f}\left(1 - c_{\tau'_c}\right)^2$$

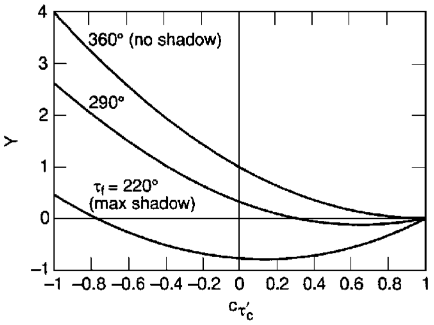

Fig. 3 Plot of function y vs cos(τ'_c) for τ_f = 220, 290, and 360 deg.

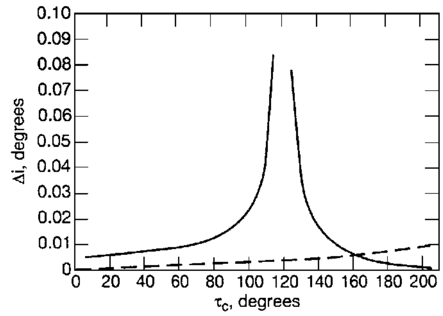

Fig. 4 Delta inclination vs τ'_c for τ_f = 220 deg and β = 60 deg.

which reduces to

$$c^2_{\tau'_c}\left(1 - c_{\tau_f}\right) - s^2_{\tau_f} c_{\tau'_c} + c_{\tau_f}\left(1 - c_{\tau_f}\right) \geq 0$$

However, $s^2_{\tau_f} = (1-c_{\tau_f})(1+c_{\tau_f})$, and because $(1-c_{\tau_f}) \geq 0$, we can divide this inequality by $(1 - c_{\tau_f})$ to obtain the following condition:

$$y = c^2_{\tau'_c} - \left(1 + c_{\tau_f}\right)c_{\tau'_c} + c_{\tau_f} \geq 0 \tag{13}$$

The roots of this quadratic are

$$c_{\tau'_c} = \frac{\left(1 + c_{\tau_f}\right) \pm \left(1 - c_{\tau_f}\right)}{2} = 1, c_{\tau_f}$$

The inequality in Eq. (13) is satisfied for $c_{\tau'_c} \leq c_{\tau_f}$ and because, in this discussion, $s_{\tau'_c} \leq 0$ or $\pi \leq \tau'_c \leq \tau_f$, $c_{\tau'_c} \leq c_{\tau_f}$ is always satisfied. In short, whether $s_{\tau'_c} \geq 0$ or $s_{\tau'_c} \leq 0$, the expression in Eq. (11) is always ≥ 0. Figure 3 shows the plot of Eq. (13) or $y = f(c_{\tau'_c})$ for three values of τ_f, namely 220, 290, and 360 deg, the latter corresponding to the case of no shadow, whereas the former is for maximum shadow. In Fig. 3, the lower parabola is for $\tau_f = 220$ deg, and the uppermost parabola is for $\tau_f = 360$ deg. The y and x abscissa intersects are of equal value.

This discussion shows then that $s_{\theta_{h_1}}$ has the same sign as $c_{\beta-\tau'_c} - c_{\beta-\tau_f}$ and $s_{\theta_{h_2}}$ has the same sign as $c_{\beta-\tau'_c} - c_\beta$ in Eqs. (9) and (10), and because $|s_{\theta_{h_1}}| \leq 1$, $|s_{\theta_{h_2}}| \leq 1$, the following conditions must be satisfied:

$$\Delta i \leq \frac{g\left(s_{\tau_f-\tau'_c} + s_{\tau'_c} - s_{\tau_f}\right)}{\left|c_{\beta-\tau'_c} - c_\beta\right|} \tag{14}$$

$$\Delta i \leq \frac{g\left(s_{\tau_f-\tau'_c} + s_{\tau'_c} - s_{\tau_f}\right)}{\left|c_{\beta-\tau'_c} - c_{\beta-\tau_f}\right|} \tag{15}$$

Then, given β and τ_f, the value of τ'_c must be such that Δi is maximized. However, because Eqs. (14) and (15) also must be satisfied, Δi is the minimum of the two maxima, namely,

$$\Delta i_1 = \frac{g\left(s_{\tau_f-\tau'_c} + s_{\tau'_c} - s_{\tau_f}\right)}{\left|c_{\beta-\tau'_c} - c_{\beta-\tau_f}\right|} \tag{16}$$

$$\Delta i_2 = \frac{g\left(s_{\tau_f-\tau'_c} + s_{\tau'_c} - s_{\tau_f}\right)}{\left|c_{\beta-\tau'_c} - c_\beta\right|} \tag{17}$$

These two functions are plotted in Fig. 4 as a function of τ'_c for $\tau_f = 220$ deg and $\beta = 60$ deg. The upper curve corresponds to Δi_2, which has singularities at $\tau'_c = 0$ and 120 deg in this case because $|c_{\beta-\tau'_c} - c_\beta| = 0$ at those values. The curve Δi_1 stays below Δi_2 until about $\tau'_c \simeq 162$ deg, after which it becomes the largest until $\tau'_c = \tau_f = 220$ deg, where it shows a singularity because $|c_{\beta-\tau'_c} - c_{\beta-\tau_f}| = 0$ there. These singularities are not worrisome because Δi must be less than the smaller of either Δi_1 or Δi_2 for a feasible solution, and those solutions always exist. From $\tau'_c = 0$ up to $\tau'_c \simeq 160$ deg (the crossover point), Δi must be less than or equal to Δi_1, i.e., $\Delta i \leq \Delta i_1$, whereas after the crossover point, $\Delta i \leq \Delta i_2$ such that Δi is less than or equal to the smaller of either Δi_1 or Δi_2. In other words, the feasible domain is the area in Fig. 4 between the x axis and the lowest branches of either curve. Clearly, there exists an optimal τ'_c ($\simeq 162$ deg in this example) such that Δi is maximized. This maximum corresponds to $\Delta i_1 = \Delta i_2$. The values of the various parameters used in Fig. 4 are $a_0 = 7000$ km, $\mu = 398{,}601.3$ km^3/s^2, and $k = 3.5 \times 10^{-7}$ km/s^2, corresponding to $g = 4.302544 \times 10^{-5}$. For given Δi, τ_f, β, and g, the location of τ'_c is uniquely defined provided that Δi corresponds to the crossover point of Δi_1 and Δi_2, where $\Delta i = \Delta i_1 = \Delta i_2$, and where $|s_{\theta_{h_1}}| = |s_{\theta_{h_2}}| = 1$. To cover both cases, namely, the sequence $\theta_{h_1} = \pi/2$, $\theta_{h_2} = -\pi/2$, and $\theta_{h_1} = -\pi/2$, $\theta_{h_2} = \pi/2$, Eqs. (7) and (8) reduce to

$$\pm g\left(2s_{\tau'_c} - s_{\tau_f}\right) = \Delta i \, c_\beta \tag{18}$$

$$\pm g\left(1 + c_{\tau_f} - 2c_{\tau'_c}\right) = \Delta i \, s_\beta \tag{19}$$

from which

$$s_{\tau'_c} = \frac{1}{2}\left(\frac{\pm\Delta i \, c_\beta}{g} + s_{\tau_f}\right) \tag{20}$$

$$c_{\tau'_c} = -\frac{1}{2}\left[\frac{\pm\Delta i \, s_\beta}{g} - \left(1 - c_{\tau_f}\right)\right] \tag{21}$$

such that

$$s_{\tau'_c} = \tan^{-1}\left[\frac{s_{\tau_f} + (\pm\Delta i/g)c_\beta}{\left(1 + c_{\tau_f}\right) - (\pm\Delta i/g)s_\beta}\right] \tag{22}$$

From Fig. 4, $\beta = 60$ deg, $\tau_f = 220$ deg, $g = 4.302544 \times 10^{-5}$, and $\Delta i = 6.1 \times 10^{-3}$ deg such that, with the plus sign selected in Eq. (22), $\tau'_c \simeq 162.7$ deg. This is clearly the unique solution because, if we select the minus sign instead, Eq. (22) will yield $\tau'_c \simeq 321.6$ deg, which is larger than τ_f and therefore not acceptable. Conversely, if we select $\tau'_c \simeq 150$ deg instead, as an example, then from Eqs. (16) and (17), $\Delta i_1 = 0.00009535$ rad and $\Delta i_2 = 0.00017919$ rad, so that, satisfying the inequalities in Eqs. (14) and (15), we can select any value of Δi provided that $\Delta i \leq \min(\Delta i_1, \Delta i_2)$ or $\Delta i \leq \Delta i_1 = 0.00009535$ rad. At $\Delta i = \Delta i_1$ exactly, Eqs. (9) and (10) yield $s_{\theta_{h_1}} = 1.0$, $s_{\theta_{h_2}} = -0.532089$, or $\theta_{h_1} = \pi/2$ and $\theta_{h_2} = -32.146$ deg. It is then clear that, for a given τ'_c different from the optimal τ'_c, any $\Delta i \leq \min(\Delta i_1, \Delta i_2)$ can be achieved with a unique combination of θ_{h_1} and θ_{h_2} with either $|\theta_{h_1}|$ or $|\theta_{h_2}| = \pi/2$ if the maximum feasible Δi is selected as described earlier, where $\Delta i = \Delta i_1$ was selected. For lower values of Δi, both θ_{h_1} and θ_{h_2} are less than $\pi/2$ in absolute value, and only at the optimal τ'_c, where $\Delta i_1 = \Delta i_2 = \Delta i$ (maximum), both $|\theta_{h_1}| = |\theta_{h_2}| = \pi/2$. If τ'_c is very close to τ_f, it may be preferable to select a smaller τ'_c for operational considerations by rotating the orbit a little bit less along the required line of nodes during the revolution. Other considerations also may limit the θ_{h_i} angles to less than a given value, for example, much less than the maximum $\pm\pi/2$, such that, once again, an appropriate τ'_c different from the optimal τ'_c would be selected.

Now, going back to the preceding discussion, it has been determined that $s_{\theta_{h_1}}$ has the same sign as $c_{\beta-\tau'_c} - c_{\beta-\tau_f}$ and that $s_{\theta_{h_2}}$

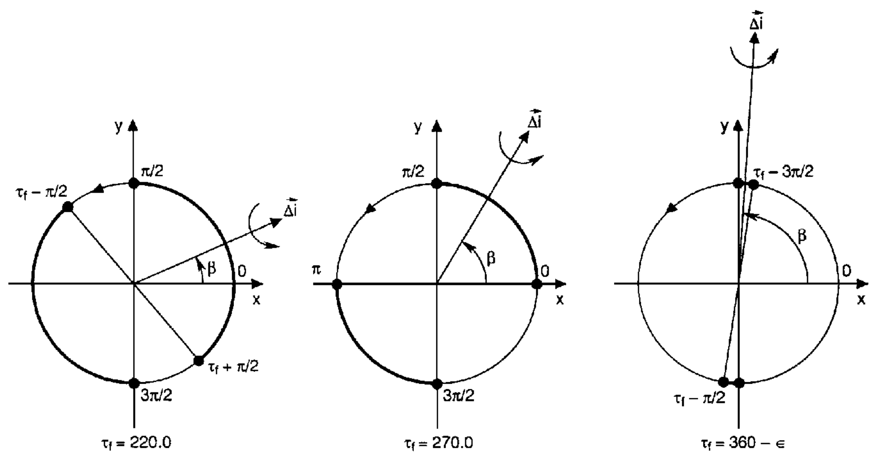

Fig. 5 Yaw angle switch regions for τ_f = 220, 270, and nearly 360 deg.

has the same sign as $c_{\beta-\tau_c'} - c_\beta$, such that $s_{\theta_{h_1}}$ and $s_{\theta_{h_2}}$ have opposite signs whenever $c_{\beta-\tau_f}$ and c_β have opposite signs. The functions c_β and $c_{\beta-\tau_f}$ for $\tau_f = 220$ deg have opposite signs for $\tau_f - 3\pi/2 \le \beta \le \pi/2$, $\tau_f - \pi/2 \le \beta \le 3\pi/2$, and $\tau_f + \pi/2 \le \beta \le 2\pi$. This is shown in Fig. 5 for three values of τ_f, namely, $\tau_f = 220$ deg (maximum shadow case), 270 deg, and 360-ε deg, where ε is small. The heavy line indicates the regions where β is such that $s_{\theta_{h_1}}$ and $s_{\theta_{h_2}}$ are of opposite sign. Where τ_f is close to 2π, as in the last case, the values of β for which $s_{\theta_{h_1}}$ and $s_{\theta_{h_2}}$ are of opposite sign are such that $\tau_f - 3\pi/2 \le \beta \le \pi/2$ and $\tau_f - \pi/2 \le \beta \le 3\pi/2$, corresponding to a very small region along the orbit. This means that, for most orientations of $\boldsymbol{\Delta i}$, θ_h will not change sign if we restrict ourselves to this single-switch theory. This in turn will be achieved at the expense of vanishingly small Δi changes because most of the thrust will be wasted to satisfy the rotation along the required line of nodes. This, then, leads us to extend this analysis to include the case in which two switches in the θ_h angle are allowed in order to be able to carry out larger changes in relative inclination along any given orientation of the line of nodes. Here, we restrict our analysis to yaw angles of 90 and −90 deg only so that the orbit remains perfectly circular at all times, while maximizing the relative inclination change along the desired line of nodes.

Algorithms of Two-Switch Transfer

Let us assume that $|\theta_{h_i}| = \pi/2$ such that the thrust vector is directed purely normal to the orbital plane. Because we are considering, at most, two switches in the yaw angle, the yaw program is therefore $\pi/2, -\pi/2, \pi/2$ or $-\pi/2, \pi/2, -\pi/2$. From Eqs. (3) and (4), it follows that

$$\Delta i_x = \pm g\left(\int_0^{\tau_{c_1}'} c_\tau \,\mathrm{d}\tau - \int_{\tau_{c_1}'}^{\tau_{c_2}'} c_\tau \,\mathrm{d}\tau + \int_{\tau_c'}^{\tau_f} c_\tau \,\mathrm{d}\tau\right) \tag{23}$$

$$\Delta i_y = \pm g\left(\int_0^{\tau_{c_1}'} s_\tau \,\mathrm{d}\tau - \int_{\tau_{c_1}'}^{\tau_{c_2}'} s_\tau \,\mathrm{d}\tau + \int_{\tau_{c_2}'}^{\tau_f} s_\tau \,\mathrm{d}\tau\right) \tag{24}$$

or

$$\Delta i_x = \pm g\left(2s_{\tau_{c_1}'} - 2s_{\tau_{c_2}'} + s_{\tau_f}\right) \tag{25}$$

$$\Delta i_x = \pm(-g)\left(2c_{\tau_{c_1}'} - 1 - 2c_{\tau_{c_2}'} + c_{\tau_f}\right) \tag{26}$$

The plus sign is used for the $\pi/2, -\pi/2, \pi/2$ sequence and the minus sign for the $-\pi/2, \pi/2, -\pi/2$ sequence. Because $\Delta i_x = \Delta i c_\beta$ and $\Delta i_y = \Delta i s_\beta$, the two expressions in Eqs. (25) and (26) can be written as

$$\Delta i_x = g\left(2s_{\tau_{c_1}'} - 2s_{\tau_{c_2}'} + s_{\tau_f}\right) = \pm\Delta i c_\beta \tag{27}$$

$$\Delta i_y = -g\left(2c_{\tau_{c_1}'} - 2c_{\tau_{c_2}'} + c_{\tau_f} - 1\right) = \pm\Delta i s_\beta \tag{28}$$

which can be further cast into the following form:

$$s_{\tau_{c_1}'} - s_{\tau_{c_2}'} = \pm(\Delta i/2g)c_\beta - (s_{\tau_f}/2) \tag{29}$$

$$c_{\tau_{c_2}'} - c_{\tau_{c_1}'} = \pm\frac{\Delta i}{2g}s_\beta - \frac{\left(1 - c_{\tau_f}\right)}{2} \tag{30}$$

Let

$$k_1 = (\Delta i/2g)s_\beta \tag{31}$$

$$k_2 = \frac{\left(1 - c_{\tau_f}\right)}{2} \tag{32}$$

$$k_3 = (\Delta i/2g)c_\beta \tag{33}$$

$$k_4 = s_{\tau_f}/2 \tag{34}$$

Then

$$s_{\tau_{c_1}'} - s_{\tau_{c_2}'} = \pm k_3 - k_4 \tag{35}$$

$$c_{\tau_{c_1}'} - c_{\tau_{c_2}'} = \pm(-k_1) + k_2 \tag{36}$$

Given the orientation of the line of nodes defined by the angle β and the magnitude of the relative inclination change Δi, as well as the normalized acceleration g, it is possible to solve for τ_{c_1}' and τ_{c_2}', the switch angular positions, from Eqs. (35) and (36). From Eq. (36),

$$\pm\left(1 - s_{\tau_{c_2}'}^2\right)^{\frac{1}{2}} = \pm\left(1 - s_{\tau_{c_1}'}^2\right)^{\frac{1}{2}} - [\pm(-k_1) + k_2]$$

squaring yields

$$\left(1 - s_{\tau_{c_2}'}^2\right) = 1 - s_{\tau_{c_1}'}^2 + [\pm(-k_1) + k_2]^2$$

$$-(\pm 2)\left(1 - s_{\tau_{c_1}'}^2\right)^{\frac{1}{2}}[\pm(-k_1) + k_2]$$

However, $s_{\tau_{c_2}'}$ can be eliminated by way of Eq. (35) because

$$s_{\tau_{c_2}'} = s_{\tau_{c_1}'} - (\pm k_3 - k_4)$$

$$s_{\tau_{c_2}'}^2 = s_{\tau_{c_1}'}^2 + (\pm k_3 - k_4)^2 - 2s_{\tau_{c_1}'}(\pm k_3 - k_4)$$

Therefore, after carrying out this elimination, one has

$$K - 2s_{\tau_{c_1}'}(\pm k_3 - k_4) = \pm 2\left(1 - s_{\tau_{c_1}'}^2\right)^{\frac{1}{2}}[\pm(-k_1) + k_2]$$

which is squared once again to yield the quadratic form

$$As_{\tau_{c_1}'}^2 + Bs_{\tau_{c_1}'} + C = 0 \tag{37}$$

where

$$K = (\pm k_3 - k_4)^2 + [\pm(-k_1) + k_2]^2 \tag{38}$$

$$A = K \tag{39}$$

$$B = -K(\pm k_3 - k_4) \tag{40}$$

$$C = -[\pm(-k_1) + k_2]^2 + (K^2/4) \tag{41}$$

The solution of Eq. (37) is

$$s_{\tau'_{c_1}} = \frac{-B \pm (B^2 - 4AC)^{\frac{1}{2}}}{2A} \tag{42}$$

Now, from Eq. (35),

$$\pm\left(1 - c^2_{\tau'_{c_2}}\right)^{\frac{1}{2}} = \pm\left(1 - c^2_{\tau'_{c_1}}\right)^{\frac{1}{2}} - (\pm k_3 - k_4)$$

and eliminating $c_{\tau'_{c_2}}$ this time from Eq. (36) and using the same manipulations that generated Eq. (37), a quadratic form in $c_{\tau'_{c_1}}$ can be obtained:

$$Ac^2_{\tau'_{c_1}} + B'c_{\tau'_{c_1}} + C' = 0 \tag{43}$$

where

$$A = K \tag{44}$$

$$B' = -K[\pm(-k_1) + k_2] \tag{45}$$

$$C' = -(\pm k_3 - k_4)^2 + (K^2/4) \tag{46}$$

The solution of Eq. (43) is

$$c_{\tau'_{c_1}} = \frac{-B' \pm (B'^2 - 4AC')^{\frac{1}{2}}}{2A} \tag{47}$$

Once τ'_{c_1} is computed, τ'_{c_2} can be obtained from Eqs. (35) and (36) such that

$$s_{\tau'_{c_2}} = s_{\tau'_{c_1}} - (\pm k_3 - k_4) \tag{48}$$

$$c_{\tau'_{c_2}} = c_{\tau'_{c_1}} - [\pm(-k_1) + k_2] \tag{49}$$

The condition $B^2 - 4AC \geq 0$ must be satisfied such that

$$B^2 - 4AC = K\left\{K(\pm k_3 - k_4)^2 + 4[\pm(-k_1) + k_2]^2 - K^2\right\} \geq 0$$

which reduces to the condition

$$K\left\{4 - [\pm(-k_1) + k_2]^2 - (\pm k_3 - k_4)^2\right\}[\pm(-k_1) + k_2]^2 \geq 0$$

However, $K \geq 0$ and the last bracket is also ≥ 0, such that the preceding condition can be replaced by the simpler condition

$$4 - [\pm(-k_1) + k_2]^2 - (\pm k_3 - k_4)^2 \geq 0 \tag{50}$$

If we choose the plus sign, which corresponds to the yaw sequence $\pi/2, -\pi/2, \pi/2$, the condition in Eq. (50) can be written as

$$y' = -x^2 + \left[s_\beta\left(1 - c_{\tau_f}\right) + c_\beta s_{\tau_f}\right]x + \left[4 - \tfrac{1}{2}\left(1 - c_{\tau_f}\right)\right] \geq 0 \tag{51}$$

The roots of this quadratic are given by

$$x = \left(\left[s_\beta\left(1 - c_{\tau_f}\right) + c_\beta s_{\tau_f}\right] \mp \left\{\left[s_\beta\left(1 - c_{\tau_f}\right) + c_\beta s_{\tau_f}\right]^2 + 4\left[4 - \tfrac{1}{2}\left(1 - c_{\tau_f}\right)\right]\right\}^{\frac{1}{2}}\right)\Big/2 \tag{52}$$

where $x = \Delta i/2g$ is proportional to Δi. Given β, g, and τ_f, we seek the maximum value of Δi that satisfies the condition in Eq. (51). The solutions given by Eq. (52) always exist because the square-root term is ≥ 0. This is because the term $4[4 - \frac{1}{2}(1 - c_{\tau_f})] \geq 0$. If $[s_\beta(1 - c_{\tau_f}) + c_\beta s_{\tau_f}] < 0$, the plus sign must be chosen in Eq. (52) so that $\Delta i > 0$ or $x > 0$. Conversely, if $[s_\beta(1 - c_{\tau_f}) + c_\beta s_{\tau_f}] > 0$, the plus sign again must be chosen to obtain x or $\Delta i > 0$. Therefore, the range of x is $0 \leq x \leq x_2$, where x_2 is given by

$$x_2 = \left(\left[s_\beta\left(1 - c_{\tau_f}\right) + c_\beta s_{\tau_f}\right] + \left\{\left[s_\beta\left(1 - c_{\tau_f}\right) + c_\beta s_{\tau_f}\right]^2 + 4\left[4 - \tfrac{1}{2}\left(1 - c_{\tau_f}\right)\right]\right\}^{\frac{1}{2}}\right)\Big/2 \tag{53}$$

Obviously, we must choose $x = x_2$ because it corresponds to the largest $\Delta i_{\max}$ that can be achieved along the required line of nodes, unless a smaller $\Delta i < \Delta i_{\max}$ is needed to fine tune the final inclination, in which case all of the coefficients are defined, leading to the solution of τ'_{c_1} and τ'_{c_2}. Choosing $x = x_2$, $y' = 0$ and therefore $B^2 - 4AC = 0$, which simplifies Eq. (42) to

$$s_{\tau'_{c_1}} = -B/2A \tag{54}$$

If $\beta = 0$ and $\tau_f = 360$ deg (no eclipse condition), $x_2 = 2$ and $\Delta i_{\max} = 4g$, which is the maximum angle by which the circular orbit can be rotated after one revolution of continuous thrusting. Going back to the condition in Eq. (5), if we now select the yaw sequence $-\pi/2, \pi/2, -\pi/2$, then that condition will reduce to

$$y' = -x^2 - \left[s_\beta\left(1 - c_{\tau_f}\right) + c_\beta s_{\tau_f}\right]x + \left[4 - \tfrac{1}{2}\left(1 - c_{\tau_f}\right)\right] \geq 0 \tag{55}$$

whose roots are given by

$$x = \left(-\left[s_\beta\left(1 - c_{\tau_f}\right) + c_\beta s_{\tau_f}\right] \mp \left\{\left[s_\beta\left(1 - c_{\tau_f}\right) + c_\beta s_{\tau_f}\right]^2 + 4\left[4 - \tfrac{1}{2}\left(1 - c_{\tau_f}\right)\right]\right\}^{\frac{1}{2}}\right)\Big/2 \tag{56}$$

Once again, if $[s_\beta(1 - c_{\tau_f}) + c_\beta s_{\tau_f}] < 0$, the plus sign must be chosen to get $\Delta i > 0$, and conversely, if $[s_\beta(1 - c_{\tau_f}) + c_\beta s_{\tau_f}] > 0$, the plus sign also must be chosen to yield $\Delta i > 0$.

The maximum $\Delta i_{\max}$ is achieved for $x = x'_2$, where x'_2 is given by

$$x'_2 = \left(-\left[s_\beta\left(1 - c_{\tau_f}\right) + c_\beta s_{\tau_f}\right] + \left\{\left[s_\beta\left(1 - c_{\tau_f}\right) + c_\beta s_{\tau_f}\right]^2 + 4\left[4 - \tfrac{1}{2}\left(1 - c_{\tau_f}\right)\right]\right\}^{\frac{1}{2}}\right)\Big/2 \tag{57}$$

and the range of x is now $0 \leq x \leq x'_2$. At $x = x'_2$, $y' = 0$, and $B^2 - 4AC = 0$ too, such that as in Eq. (54),

$$s_{\tau'_{c_1}} = -B/2A \tag{58}$$

The maximum $\Delta i_{\max}$ therefore is achieved by $\Delta i_{\max} = \max(2gx_2, 2gx'_2)$. The same discussion carried out so far for $s_{\tau'_{c_1}}$ also can be applied to $c_{\tau'_{c_1}}$ because, from Eq. (47),

$$B'^2 - 4AC' = K\left\{K[\pm(-k_1) + k_2]^2 + 4(\pm k_3 - k_4)^2 - K^2\right\} \geq 0$$

reduces to the condition

$$K\left\{4 - (\pm k_3 - k_4)^2 - [\pm(-k_1) + k_2]^2\right\}(\pm k_3 - k_4)^2 \geq 0$$

which is identical to the condition in Eq. (50). The selection of x_2 or x'_2 once again will result in $B'^2 - 4AC' = 0$; therefore, for maximum Δi,

$$c_{\tau'_{c_1}} = -B'/2A \tag{59}$$

Algorithm 1

This algorithm uses a very simple logic, as follows: Let the sequence $\pi/2$, $-\pi/2$, $\pi/2$ for the yaw angle correspond to $S = 1$ and the sequence $-\pi/2$, $\pi/2$, $-\pi/2$ correspond to $S = -1$. If $0 \le \beta < \pi/2$ and $3\pi/2 < \beta \le 2\pi$, let $S = 1$ and if $\pi/2 \le \beta \le 3\pi/2$, let $S = -1$. If $S = 1$, x_2 is computed from Eq. (53), and if $S = -1$, x_2' is computed from Eq. (57). The inclination change is evaluated next from $\Delta i = 2g x_2$ or $\Delta i = 2g x_2'$, depending on whether $S = 1$ or $S = -1$, respectively. Now, the coefficients k_1, k_2, k_3, and k_4 are evaluated from Eqs. (31), (32), (33), and (34), respectively, whereas the constants K, A, B, C, B', and C' are evaluated from Eqs. (28), (39), (40), (41), (45), and (46), respectively, with the plus sign chosen if $S = 1$ and the minus sign chosen if $S = -1$. Next, the first switch point is evaluated from $s_{\tau'_{c_1}} = -B/2A$, $c_{\tau'_{c_1}} = -B'/2A$, and the second switch point is evaluated from Eqs. (48) and (49) with, once again, the plus sign for $S = 1$ and the minus sign for $S = -1$. If $\tau'_{c_1} < \tau'_{c_2} < \tau_f$, the solution is well defined. If $\tau'_{c_2} > \tau_f$, we set $\tau'_{c_2} = \tau_f$ because this is the maximum value that it can have. However, τ'_{c_1} now must be modified to carry out the inclination change for the particular β of interest. This modification will result in a $\Delta i < \Delta i_{\max}$ because, clearly, $\Delta i_{\max}$ is not feasible in this case. To evaluate Δi and τ'_{c_1} in this case, we go back to Eqs. (48) and (49), which we write as

$$s_{\tau'_{c_1}} = \left(s_{\tau_f}/2\right) \pm (\Delta i/2g) c_\beta \tag{60}$$

$$c_{\tau'_{c_1}} = \frac{\left(1 + c_{\tau_f}\right)}{2} \pm \left(-\frac{\Delta i}{2g}\right) s_\beta \tag{61}$$

because we fixed $\tau'_{c_2} = \tau_f$. This system of equations yields the values of τ'_{c_1} and Δi such that, regardless of whether $S = 1$ or $S = -1$,

$$\tau'_{c_1} = \beta \pm \cos^{-1}\left[\tfrac{1}{2}\left(c_\beta + c_{\tau_f - \beta}\right)\right] \tag{62}$$

$$\Delta i = 2g \left\{ \left(s_{\tau'_{c_1}} - \frac{s_{\tau_f}}{2} \right)^2 + \left[\frac{\left(1 + c_{\tau_f}\right)}{2} - c_{\tau'_{c_1}} \right]^2 \right\}^{\frac{1}{2}} \tag{63}$$

The final difficulty now is choosing between the plus or minus sign in Eq. (62). Let us choose the plus sign first. If $\tau'_{c_1} > \tau_f$, then we choose the minus sign instead. If $\tau'_{c_1} > \tau_f$ still holds, then we go back to the plus sign and subtract 2π from the answer because then τ'_{c_1} also would be larger than 2π. In short, we choose the sign that yields $0 < \tau'_{c_1} < \tau_f$. When $\tau'_{c_2} = \tau_f$, there is only one switch in the angle located at τ'_{c_1}, and the solution is analogous to the one described in the preceding section with $|\theta_{h_i}| = \pi/2$. In Fig. 6, the angles τ'_{c_1} and τ'_{c_2} are given as a function of the eclipse entry angle τ_f, which defines the duration of the eclipse, for $\beta = 0$ deg. The lower curve is obviously for τ'_{c_1} and the upper curve for τ'_{c_2}. From $\tau_f = 220$ deg to about $\tau_f = 250$ deg, $\tau'_{c_2} = \tau_f$, indicating that these transfers require only one switch, given by τ'_{c_1}. For larger values of τ_f, the transfer will make use of two switches, and because $\tau_f = 360$ deg, corresponding to the case of no eclipse, $\tau'_{c_1} = 90$ deg and $\tau'_{c_2} = 270$ deg, recovering thereby the well-known solutions valid in full sunlight. All of the numerical examples studied use $a_0 = 7000$ km, $\mu = 398{,}601.3$ km^3/s^2, $k = 3.5 \times 10^{-7}$ km/s^2, and $g = 4.302544 \times 10^{-5}$, as in the preceding section.

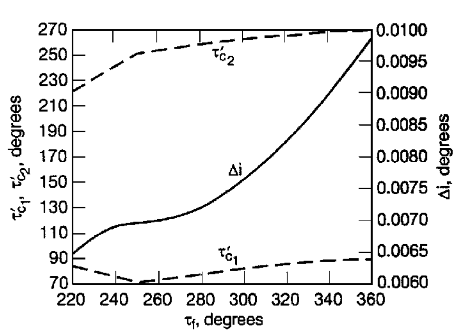

Fig. 6 Evolution of τ'_{c_1} and τ'_{c_2} and maximum change in inclination vs τ_f for $\beta = 0$ deg.

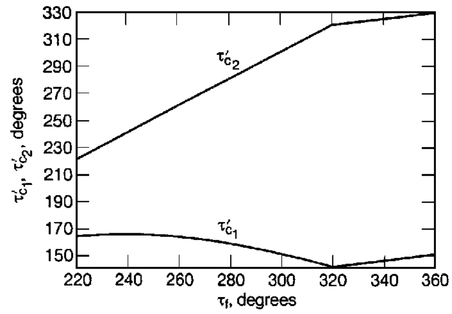

Fig. 7 τ'_{c_1} and τ'_{c_2} vs τ_f for $\beta = 60$ deg.

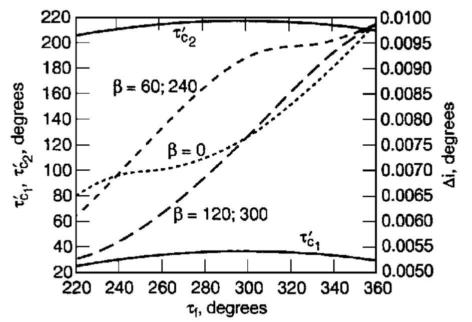

Fig. 8 τ'_{c_1} and τ'_{c_2} vs τ_f for $\beta = 120$ deg and inclination change vs τ_f for $\beta = 0$, 60, 120, 240, and 300 deg.

In Fig. 6, the maximum inclination change Δi is given as a function of τ_f for $\beta = 0$ deg. As expected, the maximum rotation takes place when $\tau_f = 360$ deg for continuous thrusting along the orbit. This maximum is $\Delta i = 9.8607 \times 10^{-3}$ deg. In Fig. 7, which corresponds to $\beta = 60$ deg, it is seen how the single-switch transfers are preponderant from $\tau_f = 220$ deg to $\tau_f = 320$ deg, after which the two-switch solutions become possible. Figure 8 is for $\beta = 120$ deg with only two-switch solutions regardless of the length of the eclipse arc. For $\beta = 240$ deg, the solutions are identical to the case in which $\beta = 60$ deg except of course $S = -1$ instead of $S = 1$. This is not surprising because $\beta \pm \pi$ and β define the same line of nodes of the initial and final orbits, the difference being that the rotations are of opposite signs, i.e., clockwise vs counterclockwise. The $\beta = 300$ deg case is identical to the case of $\beta = 120$ deg except, once again, for the sign of S. In Fig. 8, Δi is shown for these particular β values as a function of τ_f, with equal maxima at $\tau_f = 2\pi$. So far in this section, we have selected the sequence $\pi/2$, $-\pi/2$, $\pi/2$ or the sequence $-\pi/2$, $\pi/2$, $-\pi/2$ for the yaw angle, corresponding, respectively, to $S = 1$ or $S = -1$, on a purely arbitrary basis, thinking that it is very near optimal to let $S = 1$ for $3\pi/2 < \beta < \pi/2$ and $S = -1$ for $\pi/2 \le \beta \le 3\pi/2$.

Algorithm 2

This algorithm is somewhat more complex than the preceding one because it computes both solutions, namely, for $S = 1$ and $S = -1$, and compares the Δi achieved in each case. If one solution does not exist, then Δi is set to zero so that the other solution wins out. Furthermore, the two solutions, when they exist simultaneously, are not necessarily of the two-switch type, depending on β, because in many cases the second switch τ'_{c_2} becomes equal to τ_f, the eclipse entry point. As an example, for $\beta = 71$ deg, τ'_{c_1} and τ'_{c_2} are evaluated vs τ_f for the sequences $S = 1$ and $S = -1$, respectively. For this particular β, there exist indeed two distinct solutions, yielding, however, the same Δi. If β is increased to 80 deg, the two solutions will start to differ in the value of Δi that they yield because now the solution obtained with $S = -1$ provides a slightly superior Δi. Operational considerations may favor one or the other solution, depending, for example, on how fast the vehicle can be configured in attitude. At $\beta = 89$ deg, the $S = -1$ solution provides a maximum increase in Δi of about 4% over the $S = 1$ solution, showing that

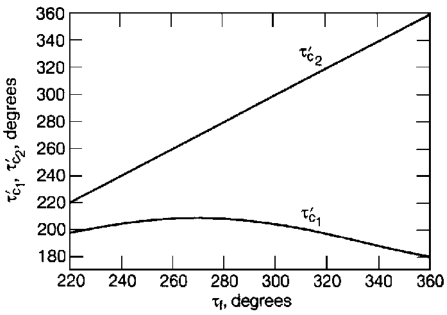

Fig. 9 τ'_{c_1} **and** τ'_{c_2} **vs** τ_f **for** β **= 89 deg and** S **= 1.**

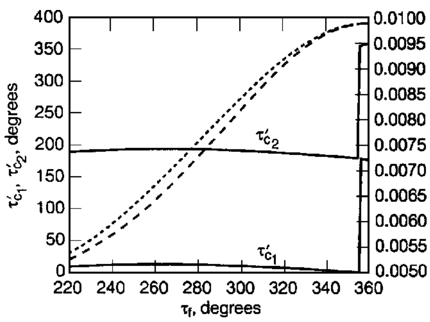

Fig. 10 τ'_{c_1} **and** τ'_{c_2} **vs** τ_f **for** β **= 89 deg and** S **= −1 and inclination change vs** τ_f **for** S **= −1 and** S **= 1 solutions.**

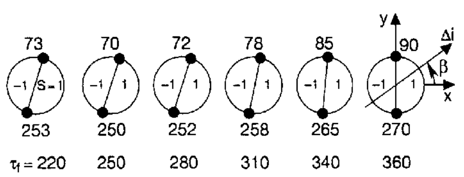

Fig. 11 S **= 1 and** S **= −1 regions of maximum** Δi **solutions in LEO vs** τ_f**.**

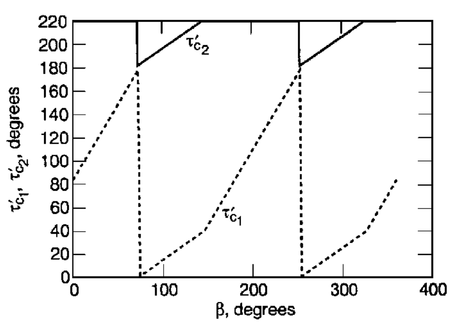

Fig. 12 **Optimal** τ'_{c_1} **and** τ'_{c_2} **vs** β **for** τ_f **= 220 deg.**

these solutions are almost equally good, as is clear from Figs. 9 and 10. This example of a LEO orbit shows that the $S = -1$ region should be extended to cover 74 deg $< \beta <$ 90 deg values at the expense of the $S = 1$ solutions. Because of symmetry, the $S = 1$ solutions now will cover the 254 deg $< \beta <$ 270 deg range as well.

Figure 11 shows that, for $\tau_f = 220$ deg, $S = 1$ for $0 \le \beta \le 73$ deg, $S = -1$ for 74 deg $\le \beta \le 253$ deg, and $S = 1$ for 254 deg $\le \beta \le 360$ deg. As τ_f approaches 360 deg, the $S = 1$ and $S = -1$ regions will tend to correspond to $\beta = 90$ and 270 deg as they should for this limiting case of no shadow. In short, Fig. 11, valid for LEO and corresponding to the most severe case of shadowing, shows how to select the yaw sequence for given τ_f and β. For example, for $\tau_f = 360$ deg, if 270 deg $\le \beta \le 90$ deg, the sequence $S = 1$ is selected; otherwise, for all other values of β, it is $S = -1$ that will yield the largest Δi. Figure 12 shows how the optimal τ'_{c_1} and τ'_{c_2} vary as a function of β for the given $\tau_f = 220$ deg. Finally, in Fig. 13, Δi vs β is plotted for various values of τ_f, namely, 220, 260, and 310 deg. The fluctuations vanish at $\tau_f = 360$ deg, and Δi becomes independent of β, displaying the constant value of 9.86×10^{-3} deg. Finally, for given β, Δi increases as τ_f is increased, as expected.

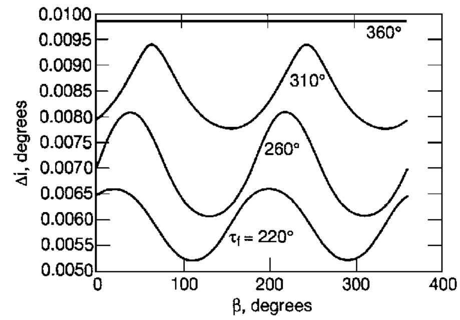

Fig. 13 **Inclination change vs** β **for** τ_f **= 220, 260, 310, and 360 deg.**

Concluding Remarks

The problem of low-thrust inclination control in near-circular orbit ($0 \le e \le 10^{-2}$) and in the presence of Earth shadow is analyzed using simple steering laws consisting of piecewise constant yaw angle selection. The linearized form of the variation-of-parameters equations is used, providing analytic expressions for the components of the inclination change vector due to out-of-plane thrusting. Two-switch transfer algorithms are analyzed, and their performances are compared. Algorithm 2, based on an optimal two-switch strategy, represents the overall better algorithm, and it provides a robust suboptimal transfer mode amenable for onboard autonomous guidance applications for future electric orbit transfer vehicles.

These algorithms are simple to implement and achieve maximum rotation of the orbital plane about the desired line of nodes of current and final orbits using constant yaw angles, with the thrust turned off during shadowing.

References

[1] Edelbaum, T. N., "Propulsion Requirements for Controllable Satellites," *ARS Journal*, Aug. 1961, pp. 1079–1089.

[2] Wiesel, W. E., and Alfano, S., "Optimal Many-Revolution Orbit Transfer," American Astronautical Society Paper 83-352, Aug. 1983.

[3] Cass, J. R., "Discontinuous Low Thrust Orbit Transfer," M.S. Thesis, School of Engineering, U.S. Air Force Inst. of Technology, AFIT/GA/AA/83D-1, Wright–Patterson AFB, OH, 1983.

[4] McCann, J. M., "Optimal Launch Time for a Discontinuous Low Thrust Orbit Transfer," M.S. Thesis, School of Engineering, U.S. Air Force Inst. of Technology, AFIT/GA/AA/88D-7, Wright–Patterson AFB, OH, 1988.

[5] Dickey, M. R., Klucz, R. S., Ennix, K. A., and Matuszak, L. M., "Development of the Electric Vehicle Analyzer," Astronautics Lab., AL-TR-90-006, U.S. Air Force Space Technology Center, Edwards AFB, CA, June 1990.

[6] Kechichian, J. A., "Low Thrust Eccentricity Constrained Orbit Raising," American Astronautical Society Paper 91-156, Feb. 1991.

[7] Kechichian, J. A., "Orbit Raising with Low Thrust Tangential Acceleration in the Presence of Earth Shadow," American Astronautical Society Paper 91-513, Aug. 1991.

[8] Sackett, L. L., Malchow, H. L., and Edelbaum, T. N., "Solar Electric Geocentric Transfer with Attitude Constraints: Analysis," Charles Stark Draper Lab., Rept. R901, Cambridge, MA, Aug. 1975.

[9] Sackett, L. L., Malchow, H. L., and Edelbaum, T. N., "Solar Electric Geocentric Transfer with Attitude Constraints: Program Manual," Charles Stark Draper Lab., Rept. R902, Cambridge, MA, Aug. 1975.

[10] Suskin, M. A., and Horsewood, J. L., "Enhancements to SECKSPOT: Convergence in the Presence of Shadowing," American Astronautical Society Paper 93-667, Aug. 1993.

[11] Marec, J. P., *Optimal Space Trajectories*, Elsevier, Amsterdam, 1979, pp. 159–168.

J. D. Gamble
Associate Editor